

Quek, L.X., et al., 2023, Southwest Borneo, an autochthonous Pangea-Eurasia assembly proxy: Insights from detrital zircon record: Geology, <https://doi.org/10.1130/G50966.1>

Supplemental Material

Figures S1–S2

Data Sets S1–S2

Data sources and methods.

1 **DATA REPOSITORY**

2 Figure S1: (A) Detrital zircon age distributions and SEM-CL images for zircon samples in
3 this study. Bin width: 20 Ma. (B) Chondrite-normalized REE patterns for zircon samples in
4 this study. Only ages of 250-200 Ma, 190-140 Ma and 140-90 Ma are plotted.
5 (C) Discriminant diagram for zircon samples in this study with continental and ocean crust
6 zircon fields defined in Grimes et al. (2007) and discriminant diagram with contrasting zircon
7 source fields defined in Wang et al. (2012). No correction has been made to the trace
8 element concentrations and the Pb concentration represents total Pb.

9 Figure S2. Large map: simplified Borneo geological map after Galin et al. (2017).
10 Samples locations for this study are indicated on the map. Small map: simplified tectonic
11 architecture of Proto-Borneo in the Mesozoic after Batara and Xu (2022), showing
12 subduction zone controlled by Proto-Tethys and Meso-Tethys.

13 Dataset S1. Detrital zircon U-Pb isotopic data

14 Dataset S2. Detrital zircon Lu-Hf isotopic data

15 Data sources and methods

16

17

GSA Supplemental Material

18

19 **Data sources and methods to accompany ‘SW Borneo, an 20 autochthonous Pangea-Eurasia assembly proxy: Insights 21 from detrital zircon record’**

22

23 Long Xiang Quek¹, Shan Li^{1*}, C.K. Morley², Azman A. Ghani³, Junbin Zhu⁴,
24 Muhammad Hatta Roselee³, Sayed Murthadha⁵, Rezal Rahmat⁶, Yu-Ming Lai⁷,
25 Ledyantje Lintjewas⁷

26 ¹*Key Laboratory of Computational Geodynamics, College of Earth and Planetary Sciences,
27 University of Chinese Academy of Sciences, 100049 Beijing, China*

28 ²*PTT Exploration and Production, Chatuchak, 10900 Bangkok, Thailand*

29 ³*Department of Geology, University Malaya, 50603 Kuala Lumpur, Malaysia*

30 ⁴*Institute of Geology, Chinese Academy of Geological Sciences, 100037 Beijing, China*

31 ⁵*Gampong Baru, Meuraxa, 23234 Banda Aceh, Indonesia*

32 ⁶*Institute of Earth Sciences, Academia Sinica, 11529 Taiwan*

33 ⁷*Department of Earth Sciences, National Taiwan Normal University, 11677 Taiwan*

34

35

36 **DATA SOURCES FOR FIGURES**

37 **Figure 1**

Data label in Excel	n	Reference
Kuching	129	
Sadong 1	130	Breitfeld et al., 2017
Sadong 2	142	
Pedawan 2	70	
Ngili 3	75	Breitfeld and Hall, 2018
Ngili 4	131	
Karimunjawa 1	107	
Karimunjawa 2	80	Witts et al., 2012
Tambak 2	92	
Kuayan	29	
Ketapang	59	
Bengkayang 1	80	Wang et al., 2022a
Bengkayang 2	71	
Bengkayang 3	79	
Kerabai	90	
Lubuk Antu 1	105	Zhao et al., 2021
Lubuk Antu 2	101	
Lubuk Antu 3	81	
Serabang 3	50	Wang et al., 2021
Serabang 1	78	
Meratus Volc	82	Wang et al., 2022b
Keramaian	69	Kueter et al., 2016

38

39

40 **Figure 2**

Data label in Excel	n	Reference
Lasipu 1	158	
Lasipu 3	91	
Lasipu 4	103	
Lasipu 5	128	
Lasipu 6	32	Zimmermann and Hall, 2019
Seical	141	
Oe Baat 1	132	
Ungar-Upper SST 1	122	
Ungar-Upper SST 2	37	
Ungar-Upper SST 4	131	
Maru 1	111	
Maru 2	123	
Maru 3	45	
Maru 4	116	
Maru 5	104	
Maru 6	126	
Maru 7	138	
Maru 8	86	
Niof 1	119	Zimmermann and Hall, 2016
Niof 2	58	
Niof 3	113	
Niof 4	77	
Niof 5	126	
Babulu 1	130	
Babulu 2	107	
Ungar	123	
Jurassic SST	133	

41

42

43

44 **METHODS**

45 **Zircon U-Pb ages and trace elements**

46 We follow the standard density and magnetic zircon separation techniques. Separated
47 zircon grains were mounted on epoxy resin and brought into a high polish. We performed the
48 measuring of U-Pb isotopes and trace elements using Laser Ablation Inductively Coupled
49 Plasma Mass Spectrometry (LA-ICP-MS) at the In-situ Mineral Geochemistry Lab, Ore
50 Deposit and Exploration Centre (ODEC), Hefei University of Technology, China. The
51 analysis instrument is an Agilent 7900 Quadrupole ICP-MS coupled to a Photon Machines
52 Analyte HE 193-nm ArF Excimer Laser Ablation system. Selection for analysis was as
53 random as possible to include all grain-size fractions and reduce preference for large zircon
54 grains. The ablation process was done in an atmosphere of UHP He (0.90 l/min), and the He
55 carrier gas (flow rate set at 0.85 l/min) carries the aerosol out of the ablation cell to the
56 plasma torch (after mixing with Ar gas immediately upon exiting). The ICP-MS system is
57 optimized daily to maximize sensitivity on isotopes of the mass range of interest while
58 keeping the production of molecular oxide species (i.e., $^{232}\text{Th}^{16}\text{O}/^{232}\text{Th}$) as low as possible,
59 and usually <0.3% (Wang et al., 2017).

60 Our analyses use standard materials 91500 (zircon) (Wiedenbeck et al., 1995) and
61 NIST610 (glass) as an external calibration for the U-Pb ages and trace element contents
62 calculation, respectively (by bracketing each block of 10 unknowns). For quality control, we
63 analyzed Plešovice zircon grains between every 10 unknown samples (Weighted mean
64 $^{206}\text{Pb}/^{238}\text{U}$ age: 335 ± 2 Ma, 2σ , n=38, is close to the reported 336 ± 1 Ma or 338 ± 1 Ma, 2σ
65 from LA ICP-MS) (Sláma et al., 2008). Each data acquisition starts with a 20 s blank, before
66 a further 40 s analysis time. Routine laser ablation conditions include a spot size of 30 μm in
67 diameter, a repetition rate of 7 Hz and an energy density of 2.5 J/cm². We performed the
68 offline data processing using ICPMSDataCal program (Liu et al., 2010). For filtered data

according to precision (10% cutoff), we use $^{238}\text{U}/^{206}\text{Pb}$ ages for zircons <1.4 Ga and $^{207}\text{Pb}/^{206}\text{Pb}$ ages for older zircons (Gehrels, 2011). And for filtered data according to discordance (10% to 30% cutoff), we use the single-grain concordia age (a type of weighted mean between the $^{206}\text{Pb}/^{238}\text{U}$ and $^{207}\text{Pb}/^{206}\text{Pb}$ ages) recommended by Vermeesch (2021) for better precision. Our kernel density estimation (KDE) plots with optimal bandwidth were done using IsoplotR (Vermeesch, 2018).

Scanning electron microscope cathodoluminescence (SEM-CL) imaging of the zircon grains was carried out using Tescan-Mira3 at Nanjing Hongchuang Geological Exploration Technology Service Co. Ltd. Through SEM-CL, we observe a high proportion of euhedral to subhedral zircon grains, with only a few rounded (Fig. DR1). The high proportion of unabraded zircon grains makes far fluvial transport doubtful; hence, they are probably mostly derived from relatively local sources. Detrital zircon grains from the samples typically show Th/U values between 1 and 0.1, which suggest that the zircon grains are mostly comparable to magmatic zircons from felsic and intermediate melt (Hoskin and Schaltegger, 2003; Linnemann et al., 2011). Only a limited amount of zircon grains shows Th/U values below 0.1, which may indicate similarity with metamorphic zircon grains. The U content of these analyzed zircon grains are high (average: ~770 ppm, max: ~4000 ppm).

86

87 Zircon Lu-Hf isotopes measurements

Concordant zircon grains were selected for in-situ Lu-Hf isotopic analyses. In-situ zircon Lu-Hf isotope analysis was measured at MRL Key Laboratory of Metallogeny and Mineral Assessment, Institute of Mineral Resources, Chinese Academy of Geological Sciences (CAGS), Beijing by using a New Wave UP213 laser-ablation microprobe, attached to a Neptune multi-collector (LA MC ICP-MS). Wu et al. (2006) described the instrumental conditions and data. We used a stationary spot, with a beam diameter of either 40 μm or 55

94 μm , depending on the size of the previously ablated domains. He carrier gas transport the
95 ablated sample from the laser-ablation cell to the ICP-MS torch via an Ar mixing chamber.
96 Chu et al. (2002) proposed ratios of $^{176}\text{Lu}/^{175}\text{Lu} = 0.02658$ and $^{176}\text{Yb}/^{173}\text{Yb} = 0.796218$ were
97 used to correct the isobaric interferences of ^{176}Lu and ^{176}Yb on ^{176}Hf . For instrumental mass
98 bias correction, Yb isotope ratios were normalized to $^{172}\text{Yb}/^{173}\text{Yb} = 1.35274$ (Chu et al.,
99 2002) and Hf isotope ratios to $^{179}\text{Hf}/^{177}\text{Hf} = 0.7325$ (Patchett and Tatsumoto, 1981) using an
100 exponential law (Albarède et al., 2004). The mass bias behavior of Lu was assumed to follow
101 that of Yb, following mass bias correction protocols detailed by Wu et al. (2006). Zircon GJ-
102 1 was our reference during routine analyses, with a weighted mean $^{176}\text{Hf}/^{177}\text{Hf}$ ratio of
103 0.282031 ± 0.000014 (2σ , $n=36$); it agrees with the weighted mean $^{176}\text{Hf}/^{177}\text{Hf}$ ratio of
104 0.282022 ± 0.000011 (2σ , $n=56$) (LA MC ICP-MS, Matteini et al., 2010).

105 We calculated the initial $^{176}\text{Hf}/^{177}\text{Hf}$ ratios, $\epsilon_{\text{Hf}}(t)$ values and model ages using the
106 zircon crystallization ages from U-Pb isotope analysis and adopting the decay constant for
107 ^{176}Lu and the chondritic ratios of $^{176}\text{Hf}/^{177}\text{Hf}$ and $^{176}\text{Lu}/^{177}\text{Hf}$, which are $1.867 \times 10^{-11}/\text{year}$
108 (Söderlund et al., 2004), and 0.282785 and 0.0336 (Bouvier et al., 2008), respectively. Our
109 calculations for the single-stage model age (T_{DM1}) relative to the depleted mantle use a
110 present-day $^{176}\text{Hf}/^{177}\text{Hf}$ ratio of 0.28325 and $^{176}\text{Lu}/^{177}\text{Hf}$ ratio of 0.0384 (Griffin et al., 2004).
111 Calculation of two-stage model ages (T_{DM2}) assumes a mean $^{176}\text{Lu}/^{177}\text{Hf}$ value of 0.015 for
112 the average continental crust (Vervoort and Blichert-Toft, 1999; Griffin et al., 2002).

113

114 **Data processing method**

115 Data is processed according to the detrital zircon age distribution fingerprinting
116 method by Barham et al. (2022) via a modified χ^2 -distribution analysis and definition of the
117 10th to 50th age percentile of the detrital zircon populations. Maximum Likelihood Age
118 (MLA) is calculated according to Galbraith and Laslett (1993) and Vermeesch (2021) and the

119 significant age peaks are calculated according to Galbraith and Green (1990). Calculations
120 are done using IsoplotR (Vermeesch, 2018).

121

122 REFERENCES CITED

- 123 Albarède, F., Telouk, P., Blichert-Toft, J., Boyet, M., Agranier, A., and Nelson, B., 2004,
124 Precise and accurate isotopic measurements using multiple-collector ICPMS1
125 1Associate editor: Y. Amelin: *Geochimica et Cosmochimica Acta*, v. 68, p. 2725–
126 2744, doi:10.1016/j.gca.2003.11.024.
- 127 Barham, M., Kirkland, C.L., and Handoko, A.D., 2022, Understanding ancient tectonic
128 settings through detrital zircon analysis: *Earth and Planetary Science Letters*, v. 583,
129 p. 117425, doi:10.1016/j.epsl.2022.117425.
- 130 Batara, B., and Xu, C., 2022, Evolved magmatic arcs of South Borneo: Insights into
131 Cretaceous slab subduction: *Gondwana Research*, v. 111, p. 142–164,
132 doi:10.1016/j.gr.2022.08.001.
- 133 Bouvier, A., Vervoort, J.D., and Patchett, P.J., 2008, The Lu–Hf and Sm–Nd isotopic
134 composition of CHUR: Constraints from unequilibrated chondrites and implications
135 for the bulk composition of terrestrial planets: *Earth and Planetary Science Letters*, v.
136 273, p. 48–57, doi:10.1016/j.epsl.2008.06.010.
- 137 Breitfeld, H.T., Hall, R., Galin, T., Forster, M.A., and BouDagher-Fadel, M.K., 2017, A
138 Triassic to Cretaceous Sundaland–Pacific subduction margin in West Sarawak,
139 Borneo: *Tectonophysics*, v. 694, p. 35–56, doi:10.1016/j.tecto.2016.11.034.
- 140 Breitfeld, H.T., and Hall, R., 2018, The eastern Sundaland margin in the latest Cretaceous to
141 Late Eocene: Sediment provenance and depositional setting of the Kuching and Sibu
142 Zones of Borneo: *Gondwana Research*, v. 63, p. 34–64, doi:10.1016/j.gr.2018.06.001.
- 143

- 144 Chu, N.-C., Taylor, R.N., Chavagnac, V., Nesbitt, R.W., Boella, R.M., Milton, J.A., German,
145 C.R., Bayon, G., and Burton, K., 2002, Hf isotope ratio analysis using multi-collector
146 inductively coupled plasma mass spectrometry: an evaluation of isobaric interference
147 corrections: *Journal of Analytical Atomic Spectrometry*, v. 17, p. 1567–1574,
148 doi:10.1039/B206707B.
- 149 Galbraith, R.F., and Green, P.F., 1990, Estimating the component ages in a finite mixture:
150 *International Journal of Radiation Applications and Instrumentation. Part D. Nuclear*
151 *Tracks and Radiation Measurements*, v. 17, p. 197–206, doi:10.1016/1359-
152 0189(90)90035-V.
- 153 Galbraith, R.F., and Laslett, G.M., 1993, Statistical models for mixed fission track ages:
154 *Nuclear Tracks and Radiation Measurements*, v. 21, p. 459–470, doi:10.1016/1359-
155 0189(93)90185-C.
- 156 Galin, T., Breitfeld, H.T., Hall, R., and Sevastjanova, I., 2017, Provenance of the Cretaceous–
157 Eocene Rajang Group submarine fan, Sarawak, Malaysia from light and heavy
158 mineral assemblages and U-Pb zircon geochronology: *Gondwana Research*, v. 51, p.
159 209–233, doi:10.1016/j.gr.2017.07.016.
- 160 Gehrels, G., 2011, Detrital Zircon U-Pb Geochronology: Current Methods and New
161 Opportunities, in *Tectonics of Sedimentary Basins*, John Wiley & Sons, Ltd, p. 45–
162 62, doi:10.1002/9781444347166.ch2.
- 163 Griffin, W.L., Belousova, E.A., Shee, S.R., Pearson, N.J., and O'Reilly, S.Y., 2004, Archean
164 crustal evolution in the northern Yilgarn Craton: U–Pb and Hf-isotope evidence from
165 detrital zircons: *Precambrian Research*, v. 131, p. 231–282,
166 doi:10.1016/j.precamres.2003.12.011.
- 167 Griffin, W.L., Wang, X., Jackson, S.E., Pearson, N.J., O'Reilly, S.Y., Xu, X., and Zhou, X.,
168 2002, Zircon chemistry and magma mixing, SE China: In-situ analysis of Hf isotopes,

- 169 Tonglu and Pingtan igneous complexes: *Lithos*, v. 61, p. 237–269,
170 doi:10.1016/S0024-4937(02)00082-8.
- 171 Grimes, C.B., John, B.E., Kelemen, P.B., Mazdab, F.K., Wooden, J.L., Cheadle, M.J.,
172 Hanghøj, K., and Schwartz, J.J., 2007, Trace element chemistry of zircons from
173 oceanic crust: A method for distinguishing detrital zircon provenance: *Geology*, v. 35,
174 p. 643 – 646, doi:10.1130/G23603A.1.
- 175 Hoskin, P.W.O., and Schaltegger, U., 2003, The Composition of Zircon and Igneous and
176 Metamorphic Petrogenesis: *Reviews in Mineralogy and Geochemistry*, v. 53, p. 27–
177 62, doi:10.2113/0530027.
- 178 Kueter, N., Soesilo, J., Fedortchouk, Y., Nestola, F., Belluco, L., Troch, J., Wölle, M.,
179 Guillong, M., Von Quadt, A., and Driesner, T., 2016, Tracing the depositional history
180 of Kalimantan diamonds by zircon provenance and diamond morphology studies:
181 *Lithos*, v. 265, p. 159–176, doi:10.1016/j.lithos.2016.05.003.
- 182 Linnemann, U., Ouzegane, K., Draren, A., Hofmann, M., Becker, S., Gärtner, A., and
183 Sagawe, A., 2011, Sands of West Gondwana: An archive of secular magmatism and
184 plate interactions — A case study from the Cambro-Ordovician section of the Tassili
185 Ouan Ahaggar (Algerian Sahara) using U–Pb–LA–ICP–MS detrital zircon ages:
186 *Lithos*, v. 123, p. 188–203, doi:10.1016/j.lithos.2011.01.010.
- 187 Liu, Y., Hu, Z., Zong, K., Gao, C., Gao, S., Xu, J., and Chen, H., 2010, Reappraisal and
188 refinement of zircon U-Pb isotope and trace element analyses by LA-ICP-MS:
189 *Chinese Science Bulletin*, v. 55, p. 1535–1546, doi:10.1007/s11434-010-3052-4.
- 190 Matteini, M., Dantas, E.L., Pimentel, M.M., and Bühn, B., 2010, Combined U-Pb and Lu-Hf
191 isotope analyses by laser ablation MC-ICP-MS: methodology and applications: *Anais
192 da Academia Brasileira de Ciências*, v. 82, p. 479–491, doi:10.1590/S0001-
193 37652010000200023.

- 194 Patchett, P.J., and Tatsumoto, M., 1981, A routine high-precision method for Lu-Hf isotope
195 geochemistry and chronology: Contributions to Mineralogy and Petrology, v. 75, p.
196 263–267, doi:10.1007/BF01166766.
- 197 Sláma, J. et al., 2008, Plešovice zircon — A new natural reference material for U-Pb and Hf
198 isotopic microanalysis: Chemical Geology, v. 249, p. 1–35,
199 doi:10.1016/j.chemgeo.2007.11.005.
- 200 Söderlund, U., Patchett, P.J., Vervoort, J.D., and Isachsen, C.E., 2004, The ^{176}Lu decay
201 constant determined by Lu–Hf and U–Pb isotope systematics of Precambrian mafic
202 intrusions: Earth and Planetary Science Letters, v. 219, p. 311–324,
203 doi:10.1016/S0012-821X(04)00012-3.
- 204 Vermeesch, P., 2018, IsoplotR: A free and open toolbox for geochronology: Geoscience
205 Frontiers, v. 9, p. 1479–1493, doi:10.1016/j.gsf.2018.04.001.
- 206 Vermeesch, P., 2021a, Maximum depositional age estimation revisited: Geoscience Frontiers,
207 v. 12, p. 843–850, doi:10.1016/j.gsf.2020.08.008.
- 208 Vermeesch, P., 2021b, On the treatment of discordant detrital zircon U–Pb data:
209 Geochronology, v. 3, p. 247–257, doi:10.5194/gchron-3-247-2021.
- 210 Vervoort, J.D., and Blichert-Toft, J., 1999, Evolution of the depleted mantle: Hf isotope
211 evidence from juvenile rocks through time: Geochimica et Cosmochimica Acta, v. 63,
212 p. 533–556, doi:10.1016/S0016-7037(98)00274-9.
- 213 Wang, Q., Zhu, D.-C., Zhao, Z.-D., Guan, Q., Zhang, X.-Q., Sui, Q.-L., Hu, Z.-C., and Mo,
214 X.-X., 2012, Magmatic zircons from I-, S- and A-type granitoids in Tibet: Trace
215 element characteristics and their application to detrital zircon provenance study:
216 Journal of Asian Earth Sciences, v. 53, p. 59–66, doi:10.1016/j.jseaes.2011.07.027.

- 217 Wang, Y. et al., 2022a, Jurassic subduction of the Paleo-Pacific plate in Southeast Asia: New
218 insights from the igneous and sedimentary rocks in West Borneo: *Journal of Asian*
219 *Earth Sciences*, v. 232, p. 105111, doi:10.1016/j.jseaes.2022.105111.
- 220 Wang, F., Ge, C., Ning, S., Nie, L., Zhong, G., and White, N.C., 2017, A new approach to
221 LA-ICP-MS mapping and application in geology: *Acta Petrologica Sinica*, v. 33, p.
222 3422–3436.
- 223 Wang, Y., Qian, X., Cawood, P.A., Ghani, A., Gan, C., Wu, S., Zhang, Y., Wang, Y., and
224 Zhang, P., 2022b, Cretaceous Tethyan subduction in SE Borneo: Geochronological
225 and geochemical constraints from the igneous rocks in the Meratus Complex: *Journal*
226 *of Asian Earth Sciences*, v. 226, p. 105084, doi:10.1016/j.jseaes.2022.105084.
- 227 Wang, Y., Zhang, A., Qian, X., Asis, J.B., Feng, Q., Gan, C., Zhang, Y., Cawood, P.A.,
228 Wang, W., and Zhang, P., 2021, Cretaceous Kuching accretionary orogenesis in
229 Malaysia Sarawak: Geochronological and geochemical constraints from mafic and
230 sedimentary rocks: *Lithos*, v. 400–401, p. 106425, doi:10.1016/j.lithos.2021.106425.
- 231 Wiedenbeck, M., Allé, P., Corfu, F., Griffin, W.L., Meier, M., Oberli, F., Quadt, A.V.,
232 Roddick, J.C., and Spiegel, W., 1995, Three Natural Zircon Standards for U-Th-Pb,
233 Lu-Hf, Trace Element and Ree Analyses: *Geostandards Newsletter*, v. 19, p. 1–23,
234 doi:10.1111/j.1751-908X.1995.tb00147.x.
- 235 Witts, D., Hall, R., Nichols, G., and Morley, R., 2012, A new depositional and provenance
236 model for the Tanjung Formation, Barito Basin, SE Kalimantan, Indonesia: *Journal of*
237 *Asian Earth Sciences*, v. 56, p. 77–104, doi:10.1016/j.jseaes.2012.04.022.
- 238 Wu, F.-Y., Yang, Y.-H., Xie, L.-W., Yang, J.-H., and Xu, P., 2006, Hf isotopic compositions
239 of the standard zircons and baddeleyites used in U–Pb geochronology: *Chemical*
240 *Geology*, v. 234, p. 105–126, doi:10.1016/j.chemgeo.2006.05.003.
- 241

- 242 Zhao, Q., Yan, Y., Zhu, Z., Carter, A., Clift, P.D., Amir Hassan, M.H., Yao, D., and Aziz,
243 J.H.A., 2021, Provenance study of the Lubok Antu Mélange from the Lupar valley,
244 West Sarawak, Borneo: Implications for the closure of eastern Meso-Tethys?
245 Chemical Geology, v. 581, p. 120415, doi:10.1016/j.chemgeo.2021.120415.
- 246 Zimmermann, S., and Hall, R., 2019, Provenance of Cretaceous sandstones in the Banda Arc
247 and their tectonic significance: Gondwana Research, v. 67, p. 1–20,
248 doi:10.1016/j.gr.2018.09.008.
- 249 Zimmermann, S., and Hall, R., 2016, Provenance of Triassic and Jurassic sandstones in the
250 Banda Arc: Petrography, heavy minerals and zircon geochronology: Gondwana
251 Research, v. 37, p. 1–19, doi:10.1016/j.gr.2016.06.001.

252

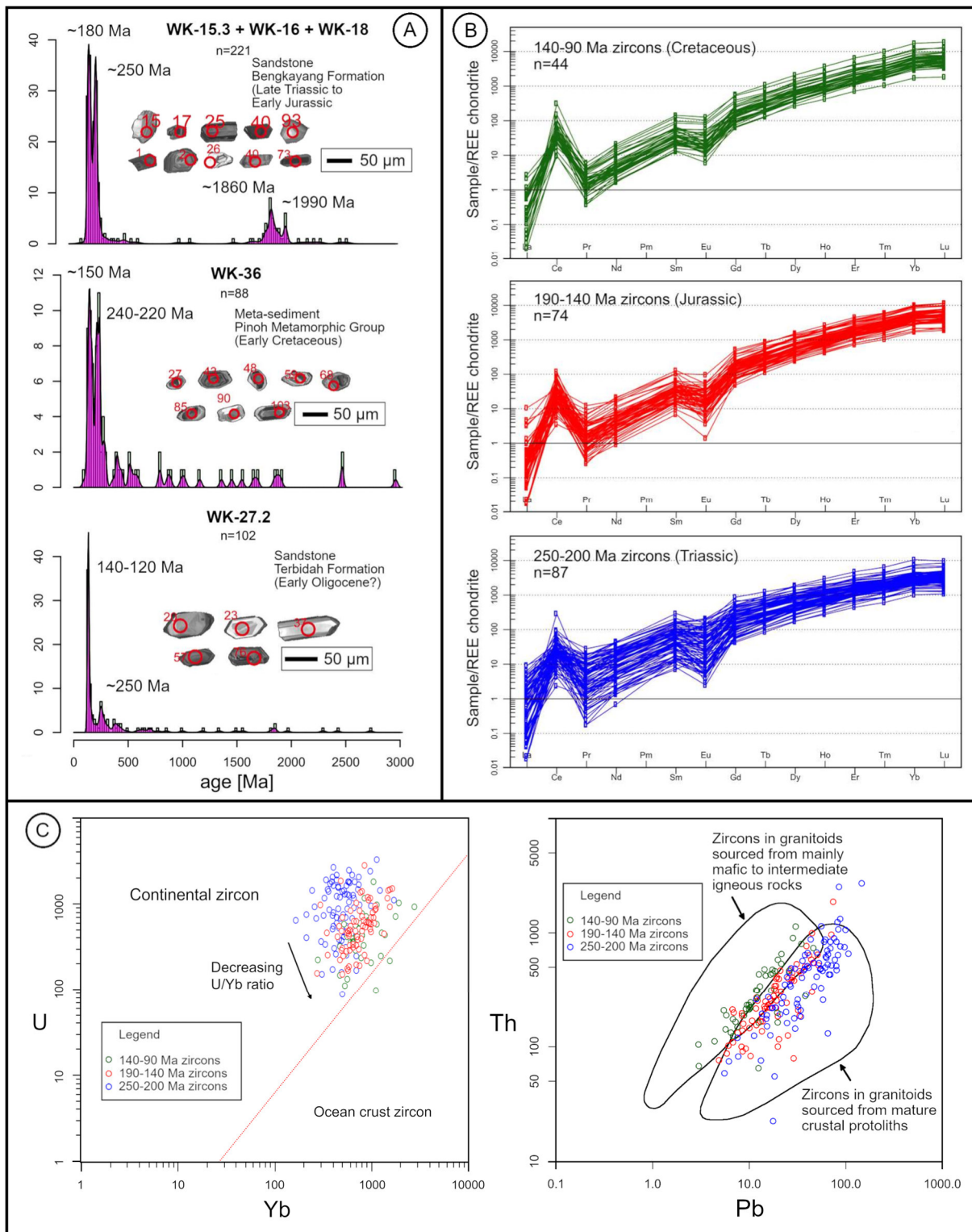
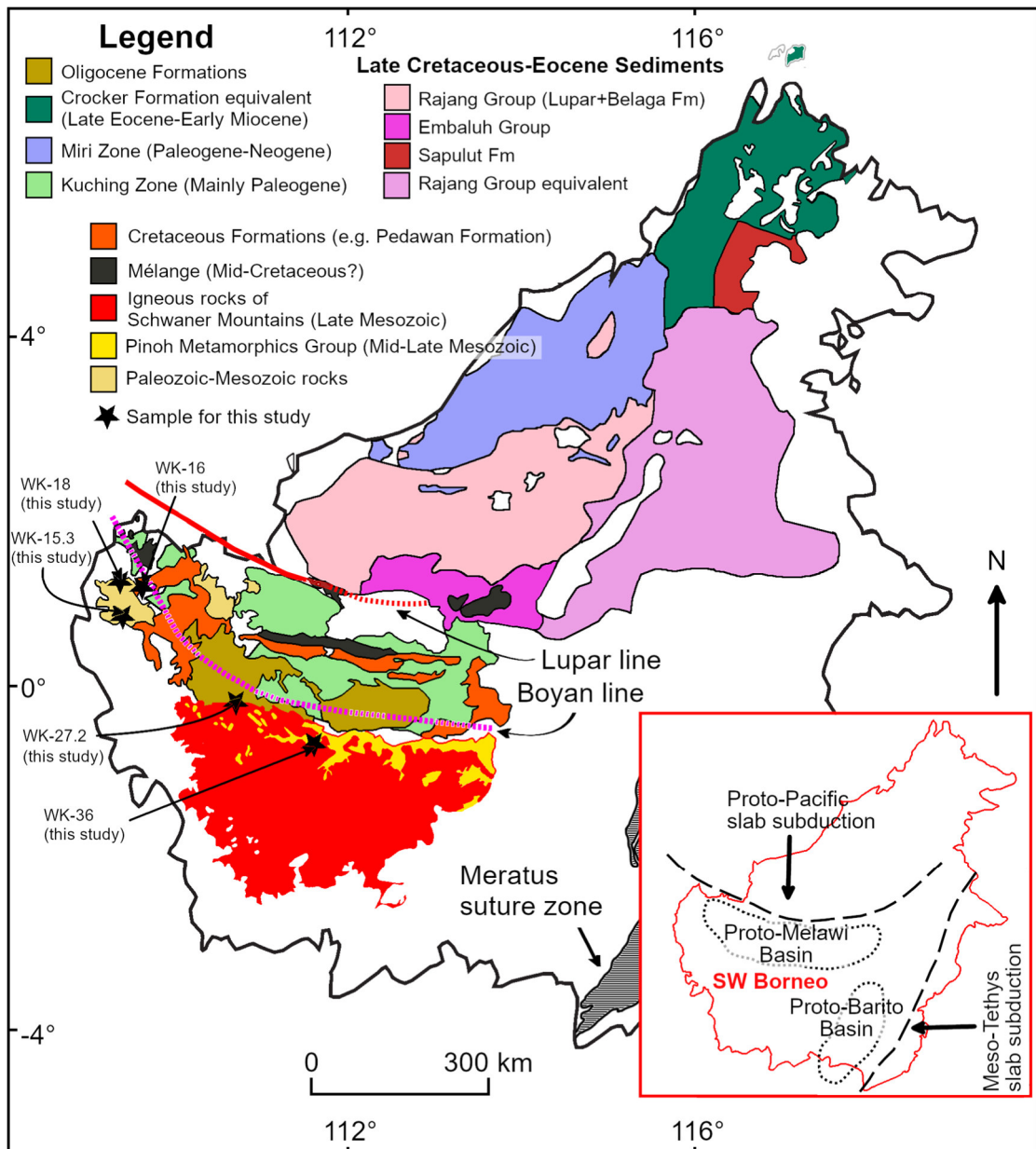


Fig. S1



255 Fig. S2

256